

The role of star formation for the galactic dynamo

Detlef Elstner¹ & Oliver Gressel²

¹Leibniz Institut for Astrophysics Potsdam, An der Sternwarte 16, 14482 Potsdam, Germany

²Astronomy Unit, Queen Mary University of London, Mile End Road, London E1 4NS, UK

Abstract

Magnetic field amplification by a fast dynamo is seen in local box simulations of SN-driven ISM turbulence, where the self-consistent emergence of large-scale fields agrees very well with its mean-field description. We accordingly derive scaling laws of the turbulent transport coefficients in dependence of the SN rate, density and rotation. These provide the input for global simulations of regular magnetic fields in galaxies within a mean-field MHD framework. Using a Kennicutt-Schmidt relation between the star formation (SF) rate and midplane density, we can reduce the number of free parameters in our global models. We consequently present dynamo models for different rotation curves and radial density distributions.

1 Introduction

Simulations of the ISM in a shearing box domain have shown that turbulence driven by SNe leads to an amplification of the mean magnetic field. Using the test-field method (Schrinner et al. 2005), we derived transport coefficients relating the mean electromotive force to the mean magnetic field (Gressel 2009). With these we were able to reproduce the time behaviour seen in the simulations. Under conditions found in our own galaxy, and assuming a constant circular velocity, a rotation rate $\gtrsim 25 \text{ Gyr}^{-1}$ was required for the dynamo to work. In order to further define the turbulence properties as a function of the star formation rate, rotation and gas density, we analysed a comprehensive set of direct simulations. Taking these as an input, we here compute global mean-field maps for a set of different model galaxies.

2 The mean-field model

Measuring test-field coefficients for a wide set of direct simulations (Gressel et al. 2008, 2011) led to the following scaling relations for the relevant diagonal term in the α tensor,

$$\alpha_{\phi\phi} = 2 \text{ km s}^{-1} \left(\frac{\sigma}{\sigma_0} \right)^{0.4} \left(\frac{\Omega}{\Omega_0} \right)^{0.5} \left(\frac{\rho}{\rho_0} \right)^{-0.1},$$

for the (downward) turbulent pumping described by the antisymmetric part of the α tensor

$$\alpha_{r\phi} = -\alpha_{\phi r} = 8 \text{ km s}^{-1} \left(\frac{\sigma}{\sigma_0} \right)^{0.45} \left(\frac{\Omega}{\Omega_0} \right)^{-0.2} \left(\frac{\rho}{\rho_0} \right)^{0.3},$$

for the turbulent diffusivity

$$\eta = 2 \text{ kpc}^2 \text{ Gyr}^{-1} \left(\frac{\sigma}{\sigma_0} \right)^{0.4} \left(\frac{\Omega}{\Omega_0} \right)^{-0.55} \left(\frac{\rho}{\rho_0} \right)^{0.4},$$

and for the mean vertical outflow velocity

$$\bar{u}_z = 15 \text{ km s}^{-1} \left(\frac{\sigma}{\sigma_0} \right)^{0.4} \frac{z}{1 \text{ kpc}}.$$

The relations were derived for SF rates, σ , varying from one tenth up to the galactic value $\sigma_0 = 30 \text{ Myr}^{-1} \text{ kpc}^{-2}$, angular velocities between $\Omega_0 = 25 \text{ Gyr}^{-1}$ and $10\Omega_0$ and midplane densities from $0.1\rho_0$ up to $\rho_0 = 1 \text{ cm}^{-3}$. From the simulations, we moreover found a vertical gradient of the turbulent velocity $\nabla_z u' = 40 \text{ km s}^{-1} \text{ kpc}^{-1}$ independent of the star formation rate, density and angular velocity.

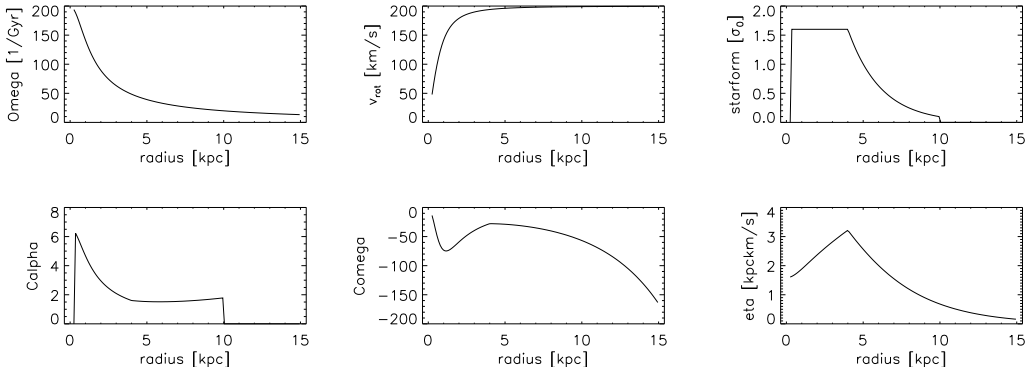


Figure 1: Radial profiles of the rotation curve, the star formation rate and the corresponding distribution of the dynamo numbers and the turbulent diffusivity for model B1 of Table 1.

We approximate the vertical profiles for the α tensor by a $\sin(2\pi z/h)$ curve with a scale height of $h = 1 \text{ kpc}$. The value of $\eta(z)$ is chosen to be constant for $-1.5h < z < 1.5h$ and linearly growing with a slope of one third outside this range. For simplicity, we assume a constant scale height within our models. We also neglect the anisotropic part of the turbulent diffusivity, which seems to be of minor importance for the current models. The rotation curve is modelled with a Brandt law

$$\Omega = \Omega_0 (1 + (r/r_\Omega)^2)^{-0.5}.$$

Further we modify the vertical wind above h by adding a radial outward velocity of the same size as \bar{u}_z . The wind velocities reach values of 100-200 km/s at $z=4\text{kpc}$, which is an order of magnitude higher than in the models of Moss et al. 2010. With these input parameters, we solve the induction equation

$$\frac{\partial \vec{B}}{\partial t} = \text{curl} \left(\vec{u} \times \vec{B} + \alpha \vec{B} - \eta \text{curl} \vec{B} \right)$$

in a cylindrical domain with $r < 15 \text{ kpc}$, and of vertical extent $-4 \text{ kpc} < z < 4 \text{ kpc}$. Defining $C_\alpha = \alpha h \eta^{-1}$ and $C_\Omega = \Omega_0 h^2 \eta^{-1}$, we obtain a dynamo number $D \equiv C_\alpha C_\Omega \propto \Omega^{2.5} \rho^{-0.9} \sigma^{-0.4}$. The pitch angle, p , can be estimated by $\tan(p) \propto (C_\alpha/C_\Omega)^{0.5}$, scaling as $\Omega^{-0.25} \rho^{-0.05} \sigma^{0.2}$. These estimates show that stronger SF reduces the dynamo number and increases the pitch

angle. It is known that the stationary quadrupole solution of the $\alpha\Omega$ dynamo exists only in a finite range of the dynamo number. Because the final strength of the regular field also depends on the saturation process, this estimate does, however, not provide a prediction for the final field strength in dependence of the star formation. Nevertheless, this behaviour still opens the possibility for radially extended regular magnetic fields. This is because, in an exponential disc, SF decays much faster with radius than the angular velocity, and hence the dynamo number may be nearly constant over a large radial range. Applying a Kenicutt Schmidt-type

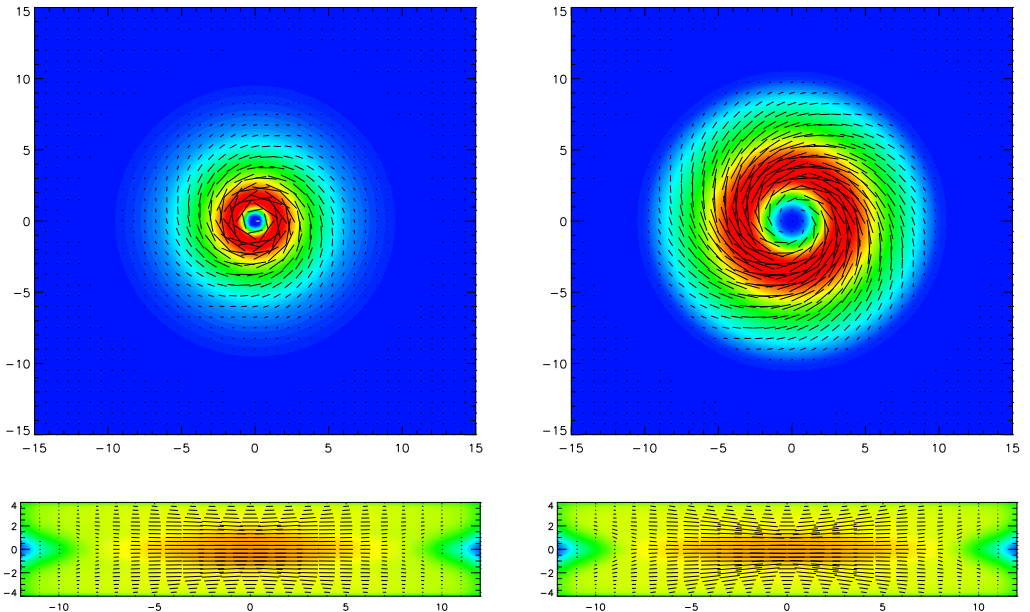


Figure 2: Total intensity (colour coded) and magnetic field vectors for model A2 and A4 of Table 1.

law, $\sigma \propto \rho^{1.4}$, we can specify our galaxy model by a radial density profile, which we leave constant up to r_ρ and then exponentially decay with a scale length of 3 kpc, as seen in Fig. 1. For the nonlinear back-reaction, we use a classical, however anisotropic, α quenching. While the usual quenching of only the diagonal terms in the α tensor would lead to solutions with a small pitch angle, independently quenching the pumping term can also saturate the dynamo by the increasing field advection from the wind. In this case, the pitch angle of the kinematic mode can be preserved (Eltner et al. 2009).

3 Results

The models rely on a crude approximation of the vertical profiles for the turbulent transport coefficients, which still leave some uncertainty in the absolute numbers given in Table 1. Nevertheless, the general trend agrees well with the predictions from the local dynamo number analysis. The pitch angle, measured from the magnetic vectors (see Fig. 2) of the polarisation map at r_ρ , increases slightly with the star formation rate as predicted by the ratio C_α/C_Ω

above. The growth times of the order of 100 Myr tend to increase with the star formation rate, but there are exceptions (cf. A1 and A2 of Table 1). No large-scale magnetic field amplification was observed for $\sigma > 10\sigma_0$ in model B3, and in the weakly differentially rotating model A5. Yet, strong starbursts are usually not long-lasting events and therefore the dynamo may still operate on longer time scales. The final field strength is not strongly dependent on the SF rate, and only the toroidal field is influenced by the difference in turbulent diffusivity. The inverse dependence of the dynamo action on the SF activity is mainly due to an enhanced

Table 1: Model parameters and results

	r_Ω [kpc]	r_ρ [kpc]	σ [σ_0]	$D(r_\Omega)$	B_φ [B_{eq}]	B_r [B_{eq}]	pitch [deg]	atan $\sqrt{C_\alpha/C_\Omega}$ [deg]	t_G [Gyr]
A1	1	7	0.4	1540	1.3	0.25	12	12	0.18
A2	1	7	1	550	1.1	0.25	14	14	0.16
A3	1	7	2.6	192	0.95	0.25	17	17	0.25
A4	2.5	7	1	86	0.65	0.28	19	19	0.35
A5	5	7	1	23	0.0001	0.0001	-	38	∞
B1	1	4	1.6	344	1.1	0.26	11	14	0.18
B2	1	4	4.2	121	0.9	0.23	13	16	0.49
B3	1	4	11.2	43	0.0001	0.0001	-	27	∞
B4	2.5	4	1.6	54	0.6	0.25	17	20	0.47

turbulent diffusion. This does not necessarily increase the turbulent velocity but may equally change the correlation time. In fact, the preference of magnetic arms *between* the optical arms may be based on this very property of ISM turbulence (cf. Rohde et al. 1999).

The main conclusions drawn from the presented set of simulations are as follows:

- SF rate and rotation determine the dynamo – calling for adequate galaxy evolution models.
- Low star formation rates favour the dynamo, explaining coherent inter-arm fields.
- Strong SF may suppress large-scale dynamo action (no vertical fields in the centre).
- Explaining the radio-FIR relation will require a different type of amplification mechanism – at least for the small-scale field.

Acknowledgements. This work was supported by a DFG grant within the research unit 1254.

References

- Elstner D., Gressel O., Rüdiger G., 2009, IAUS 259, 467
 Gressel O., Elstner D., Ziegler U., Rüdiger G., 2008, A&A 486, L35
 Gressel O., 2009, PhD thesis, University of Potsdam (astro-ph:1001.5187)
 Gressel O., Elstner D., Rüdiger G., 2011, IAUS 274, 348
 Moss D., Sokoloff D., Beck R., Krause M., 2010, A&A 512, A61
 Rohde R., Elstner D., Beck R., 1999, A&A 350, 423
 Schrinner M., Rädler K.-H., Schmitt D. et al., 2005, AN 326, 245